



Cite this: DOI: 10.1039/d5gc06335c

## Demonstrating a butylamine-based deconstruction method for poplar biomass and conversion by diverse microbial strains

 Jiayuan Jia,<sup>†a,b</sup> Demian Dietrich,<sup>†a,c</sup> Venkataramana R. Pidatala,<sup>a,d</sup> Emine Akyuz Turumtay,<sup>a,d</sup> Edward E. K. Baidoo,<sup>a,d</sup> Carolina A. Barcelos,<sup>d,e</sup> Joseph Palasz,<sup>d</sup> Md Maksudur Rahman,<sup>a,c</sup> Chae Won Kang,<sup>a,d</sup> Valentina E. Garcia,<sup>id a,c</sup> Edward Koleski,<sup>a,e</sup> Justin Panich,<sup>a,e</sup> Eric R. Sundstrom,<sup>id d,e</sup> Aymerick Eudes,<sup>id a,f</sup> Hemant Choudhary,<sup>id a,c</sup> Taek Soon Lee,<sup>a,d</sup> John M. Gladden,<sup>id a,c</sup> Blake A. Simmons,<sup>id a,d</sup> Joonhoon Kim<sup>a,b</sup> and Alberto Rodriguez<sup>id \*a,c</sup>

Low-boiling alkylamines such as butylamine offer promise as effective biomass pretreatment solvents that can be readily recovered and recycled; however, their capability to support microbial conversion of nutrients present in hydrolysates represents an important area for investigation. Here we employed butylamine to pretreat poplar biomass and characterize its effects on the release of fermentable sugars after solvent removal and enzymatic hydrolysis, as well as the biocompatibility of the produced hydrolysates with three organisms commonly used as bioconversion hosts. We observed that residual butylamine and the derivative butylacetamide were present in high enough concentrations to exert toxicity to strains of *Aspergillus niger*, *Pseudomonas putida*, and *Rhodospiridium toruloides* that produce malic acid, isoprenol and bisabolene, respectively. Removal of the toxic compounds by charcoal filtration and nutrient supplementation resulted in a hydrolysate containing >100 g L<sup>-1</sup> of sugars that enabled strong growth, substrate consumption and bioproduct accumulation, outperforming defined cultivation media. This is the first demonstration of a butylamine-based deconstruction process for poplar biomass at a pilot-scale to achieve conversion of high sugar concentrations to valuable bioproducts with engineered microbes.

 Received 25th November 2025,  
Accepted 23rd March 2026

DOI: 10.1039/d5gc06335c

[rsc.li/greenchem](http://rsc.li/greenchem)

### Green foundation

1. This work demonstrates a scalable butylamine pretreatment strategy that generates high sugar hydrolysates from poplar while enabling direct microbial conversion by fungi, bacteria, and yeast. By integrating pretreatment, detoxification, and fermentation, it establishes a unified and versatile platform for lignocellulosic bioprocessing with solvent recycling potential.
2. Pilot scale butylamine pretreatment released >100 g L<sup>-1</sup> sugars and required only minimal supplementation for *Aspergillus niger*, *Pseudomonas putida*, and *Rhodospiridium toruloides* to produce malic acid, isoprenol, and bisabolene. Activated charcoal removed inhibitory amide byproducts while preserving fermentable carbon, enabling high bioproduct titers without washing steps or energy intensive solvent recovery.
3. The approach can be further improved by reducing amide formation during pretreatment, increasing solvent recovery efficiency, and enhancing microbial tolerance to residual compounds. These refinements would streamline hydrolysate preparation and support integration with fed-batch or continuous fermentation systems.

## Introduction

Lignocellulosic biomass is the most abundant renewable resource for the sustainable production of biofuels and bioproducts.<sup>1,2</sup> Its large-scale utilization is critical for reducing dependence on finite fossil resources and enabling a national circular bioeconomy.<sup>3-5</sup> Compared to other organic waste streams, lignocellulosic biomass offers higher availability, lower competition with food systems, and a more stable

<sup>a</sup>Joint BioEnergy Institute, Emeryville, CA 94608, USA. E-mail: alberto@lbl.gov

<sup>b</sup>Pacific Northwest National Laboratory, Richland, WA 99352, USA

<sup>c</sup>Sandia National Laboratories, Livermore, CA 94550, USA

<sup>d</sup>Biological Systems and Engineering Division, Lawrence Berkeley National Laboratory, 1 Cyclotron Rd, Berkeley, CA, 94720, USA

<sup>e</sup>Advanced Biofuels and Bioproducts Process Development Unit, Emeryville, CA, USA

<sup>f</sup>Environmental Genomics and Systems Biology Division, Lawrence Berkeley National Laboratory, 1 Cyclotron Rd, Berkeley, CA, 94720, USA

<sup>†</sup>These authors contributed equally to this work.


carbon composition.<sup>6</sup> However, its conversion to fermentable substrates is hindered by restricted accessibility due to the tightly bound structure of its cell wall components: cellulose forms crystalline microfibrils encased by hemicellulose and encrusted with lignin.<sup>4,6</sup> These barriers make efficient pretreatment essential to liberate fermentable sugars and enable downstream microbial conversion. Overcoming this intrinsic recalcitrance remains one of the key technical challenges in developing scalable, cost-effective bioprocesses for lignocellulosic biomass valorization.

Various physical, chemical, and biological pretreatment technologies have been developed for lignocellulosic biomass.<sup>4,6</sup> Among these, chemical pretreatment is considered a distinctive and promising approach, including alkaline treatments, dilute acid hydrolysis, organosolv processes with organic solvents, ionic liquids (ILs), and deep eutectic solvents (DES).<sup>6–9</sup> However, most chemical pretreatments generate compounds that can be inhibitory during fermentation (e.g., furfural and 5-hydroxymethylfurfural from acid pretreatment; lignin-derived phenolics from alkaline pretreatment) and often require subsequent washing of solids and energy-intensive solvent recovery steps.<sup>10,11</sup> An ideal pretreatment solvent would efficiently break down biomass to maximize fermentable sugar yields while minimizing the formation of inhibitory byproducts, reducing the need for extensive washing or neutralization, and enabling easy solvent recovery.<sup>11,12</sup>

Amine-functionalized solvents, such as butylamine, have shown great promise for lignocellulosic biomass pretreatment due to their high deconstruction efficiency and ease of recovery.<sup>13–15</sup> Butylamine pretreatment selectively cleaves ester linkages in lignin–carbohydrate complexes, improving enzyme accessibility and enabling the release of up to 90% of cellulose-derived glucose after enzymatic hydrolysis.<sup>16,17</sup> It has outperformed other amines by delivering high fermentable sugar yields, enabling efficient solvent recovery *via* distillation, and allowing direct enzymatic hydrolysis without washing, thereby potentially simplifying downstream processing.<sup>16</sup>

Several microbial species spanning bacteria, yeasts and filamentous fungi have been studied for use in downstream processing due to their innate capacity to metabolize lignocellulose-derived substrates.<sup>18–20</sup> For instance, the filamentous fungus *Aspergillus niger*, long used for organic acid fermentations, has been engineered to efficiently convert inexpensive, unrefined substrates into L-malic acid.<sup>21</sup> Likewise, *Pseudomonas putida* has emerged as a robust bacterial host for biosynthesis of valuable compounds like the aviation fuel precursor isoprenol.<sup>22</sup> Engineered *P. putida* strains can co-consume mixed sugars, organic acids and lignin-derived molecules without compromising isoprenol production, underscoring metabolic versatility on complex feedstocks.<sup>23</sup> In the same way, the oleaginous yeast *Rhodospiridium toruloides* has been employed for terpenes (e.g. bisabolene) production, capitalizing on its high lipid accumulation capacity and innate tolerance to lignocellulosic hydrolysate inhibitors.<sup>24</sup> However, different microbial species may exhibit distinct tolerances to pretreatment inhibitors and display different nutritional

requirements and uptake mechanisms, influencing their ability to assimilate and valorize nutrients present in biomass hydrolysates.<sup>25,26</sup> Directly comparing these attractive bioconversion hosts on a standardized lignocellulosic hydrolysate could elucidate their relative strengths and guide the selection and optimization of microbial chassis in future bioprocess designs.

In this work, we evaluate the effectiveness of using a butylamine-based process that includes deconstruction, solvent removal, and microbial conversion of poplar biomass, which is an important and abundant bioenergy crop.<sup>27</sup> We assess the pretreatment efficiency by determining enzymatic saccharification yields and investigate the ability of three engineered strains of *A. niger*, *P. putida*, and *R. toruloides*, to grow in butylamine-derived hydrolysates and produce valuable bioproducts: malic acid, isoprenol, and bisabolene, respectively. By integrating pretreatment performance with microbial growth and product formation, this study provides insights into the feasibility of alkylamine-based bioconversion platforms for poplar biomass and informs microbial strain selection for future lignocellulosic bioprocess development.

## Results and discussion

### Hydrolysate characterization

Hybrid poplar was selected as a representative lignocellulosic feedstock due to its abundance and relevance for bioenergy applications. Compositional analysis of the poplar biomass indicated the following percentages for the main polymeric components: glucan ( $44.6 \pm 0.6$ ), xylan ( $20.3 \pm 0.2$ ), acid-insoluble lignin ( $28.1 \pm 0.7$ ) and acid soluble lignin ( $5.0 \pm 0.1$ ). To generate enough hydrolysate for bioconversion assays, the biomass was pretreated in a single run using a 10 L reactor using neat butylamine as the solvent (15% solids loading, 140 °C, 3 h). The pretreatment reaction was followed by a solvent removal step (80 °C, 12 h), which accomplished 93% removal efficiency. Enzymatic hydrolysis of the pretreated and dried biomass (pH 5, 50 °C, 72 h) resulted in hydrolysates containing  $77.3 \text{ g L}^{-1}$  of glucose and  $27.1 \text{ g L}^{-1}$  of xylose as the main fermentable sugars, representing saccharification yields of 88.7% and 66.8%, respectively. The obtained composition and sugar yield values proved to be analogous to those obtained after deconstructing a different type of hybrid poplar under similar reaction conditions at smaller scales,<sup>17</sup> showcasing the robustness of the butylamine-based process. Importantly, we did not detect the presence of the microbial inhibitors furfural and 5-hydroxymethylfurfural in the hydrolysate, which are commonly produced in acidic conditions at high temperatures.<sup>28</sup> This is the first report of butylamine pretreatment of poplar in a pilot scale reactor, allowing for the generation of a hydrolysate that contains a total of  $104 \text{ g L}^{-1}$  of fermentable sugars available for bioconversion, the highest reported concentration obtained with an alkylamine-based biomass conversion process. This result shows the benefits of using biomass with high glucan content like poplar combined



with pretreatment using a volatile solvent, eliminating the need for biomass washing prior to enzymatic hydrolysis that typically results in sugar losses.

### Hydrolysate biocompatibility assessment

The ability of microbial conversion hosts to tolerate lignocellulosic hydrolysates is a critical determinant of process efficiency, particularly when inhibitory compounds generated during pretreatment are not removed prior to fermentation. Therefore, we examined the tolerance of *A. niger*, *P. putida*, and *R. toruloides* to hydrolysates derived from butylamine-pretreated poplar (Fig. 1).

Growth responses across a range of hydrolysate concentrations (10–50%, v/v in the control medium) were assessed to determine strain-specific thresholds for toxicity and establish the suitability of the hydrolysate for microbial conversion. Higher hydrolysate fractions (up to 90% v/v) were evaluated but did not support growth and were therefore excluded. As shown in Fig. 1, the three strains exhibited markedly different tolerance profiles. *A. niger* displayed an intermediate tolerance (Fig. 1A). At 10% hydrolysate concentration, the fungus showed increased biomass production compared to the control, hinting that the extra nutrients in the diluted hydrolysate can initially stimulate growth. However, the growth dropped significantly at 20% hydrolysate concentration and was almost completely inhibited at 30% concentration.

*P. putida* maintained robust growth even at comparably high hydrolysate concentrations (Fig. 1B). As observed with *A. niger*, the OD<sub>600</sub> value obtained in 10% hydrolysate exceeded that of the control, suggesting that low levels of hydrolysate supply additional nutrients that *P. putida* can utilize. Growth remained substantial at 20% concentrations, with a continuous increase in biomass compared to 10% hydrolysate. A sharp decline in *P. putida* biomass was observed between 30%

to 50% hydrolysate, indicating that beyond a threshold concentration, inhibitory compounds begin to reduce the viability of this strain.

Lastly, *R. toruloides* was unable to grow even in the lowest hydrolysate concentration (Fig. 1C), suggesting that this yeast is particularly vulnerable to inhibitory compounds present in the hydrolysate. Collectively, these results highlight strain-specific differences in hydrolysate tolerance, with *P. putida* exhibiting the highest tolerance and *R. toruloides* the lowest tolerance to butylamine-treated poplar.

### Hydrolysate detoxification

Given the strain-specific growth inhibition observed in raw hydrolysates, we analyzed their chemical composition to identify potential inhibitory compounds. These compounds, even in low quantities, may disrupt membrane integrity, interfere with cellular metabolism, or exacerbate redox stress.

LC-MS analysis of the biomass hydrolysate (Fig. 2 and Table S1) identified the presence of residual butylamine (0.8 g L<sup>-1</sup>) and its acetylated byproduct butylacetamide (7.1 g L<sup>-1</sup>), along with several phenolic compounds (<1 g L<sup>-1</sup>) with known microbial toxicity including 4-hydroxybenzoic acid, syringic acid and vanillic acid.<sup>29</sup> Consistent with previous results, amidation reactions occurred under the pretreatment conditions, resulting in the formation of amide derivatives of these aromatics (in this case, *N*-butyl-4-hydroxybenzamide).<sup>17</sup> Consequently, activated charcoal was used as an adsorptive detoxification agent to reduce the concentration of these inhibitors.<sup>30–32</sup> Treatment with charcoal resulted in visible decolorization of the hydrolysate (Fig. S1). Subsequent LC-MS quantification confirmed that phenolic compounds, including both native and amidated forms, were almost entirely removed (Fig. 2). The concentration of butylacetamide was reduced by over 94% to 0.4 g L<sup>-1</sup> while butylamine showed a reduction of

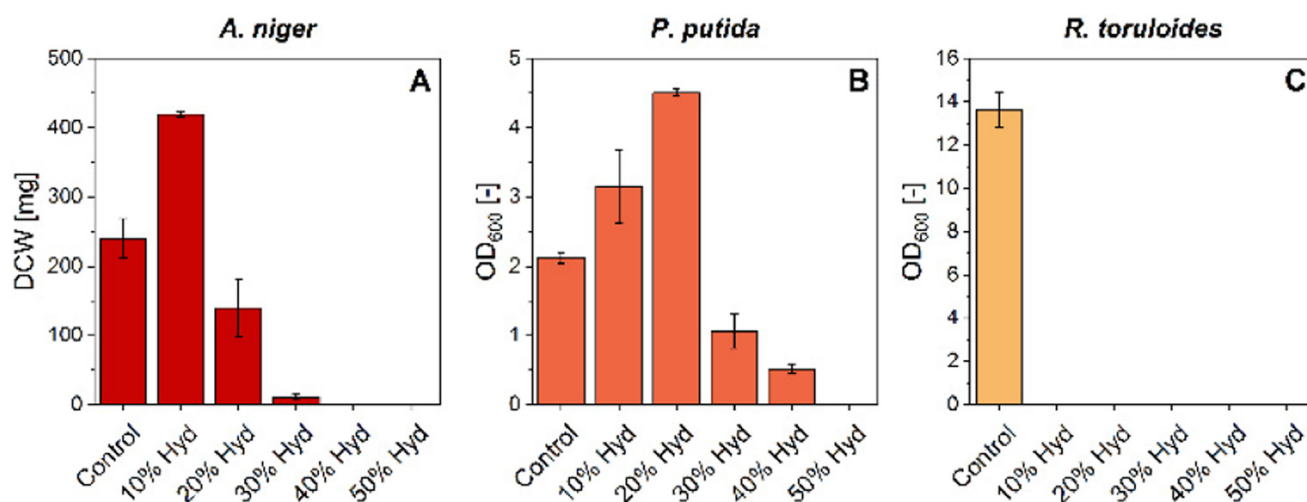


**Fig. 1** Evaluation of the microbial toxicity of the butylamine-pretreated poplar hydrolysate. The organisms were inoculated in different concentrations of hydrolysate, diluted with CM for *A. niger* (A), LB for *P. putida* (B) and YPD for *R. toruloides* (C). The biomass generation was assessed after 3 days in shake flasks by mycelial dry cell weight for *A. niger* or OD<sub>600</sub> for *P. putida* and *R. toruloides*. The data represent averages and the error bars represent standard deviations of biological triplicates ( $n = 3$ ).



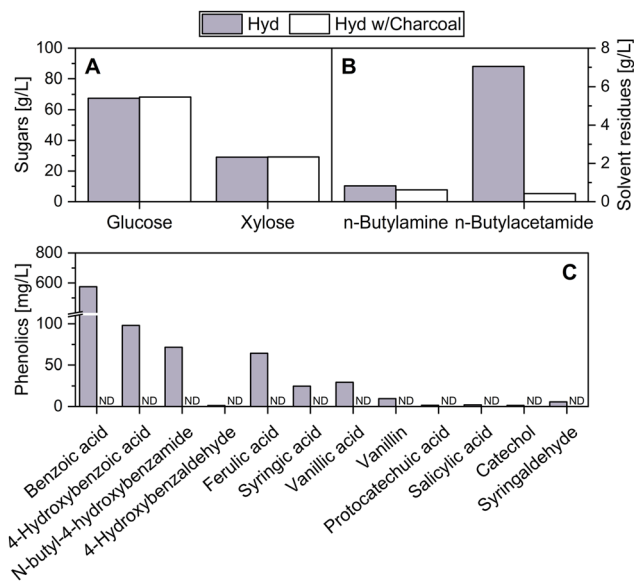


**Fig. 2** Effect of charcoal treatment on hydrolysate composition. Untreated hydrolysate (Hyd, grey) and hydrolysate after charcoal treatment (Hyd w/charcoal, white). (A) Sugar concentrations (glucose and xylose) in untreated hydrolysate (Hyd) and hydrolysate after charcoal treatment (Hyd w/charcoal). (B) Residual solvent concentrations of *n*-butylamine and *n*-butylacetamide. (C) Phenolic compounds in untreated hydrolysate, showing substantial reduction or complete removal of several phenolic inhibitors. ND = not detected; *n* = 1.

approximately 27% to  $0.6 \text{ g L}^{-1}$ . Importantly, the concentrations of fermentable sugars remained unchanged following charcoal treatment (Fig. 2A). This result is consistent with prior reports of selective adsorption of compounds with higher hydrophobicity than carbohydrates such as furans and phenolics.<sup>31</sup>

Since the detoxified hydrolysate contained only residual levels of butylamine ( $0.61 \text{ g L}^{-1}$ ) and butylacetamide ( $0.42 \text{ g L}^{-1}$ ), we assessed the biological inhibitory effects of these compounds in dose–response assays for *A. niger*, *P. putida*, and *R. toruloides* (Fig. 3). The residual concentrations of butylamine and butylacetamide were compared to the respective  $\text{IC}_{50}$  values obtained for each strain. Before charcoal treatment, the concentration of butylacetamide ( $7.1 \text{ g L}^{-1}$ ) exceeded the  $\text{IC}_{50}$  for all three strains:  $1.58 \text{ g L}^{-1}$  for *A. niger*,  $3.00 \text{ g L}^{-1}$  for *P. putida*, and  $1.47 \text{ g L}^{-1}$  for *R. toruloides*, indicating that it was likely a contributor to hydrolysate toxicity. In contrast, the concentration of butylamine was  $0.8 \text{ g L}^{-1}$ , which surpassed the  $\text{IC}_{50}$  for *R. toruloides* ( $0.67 \text{ g L}^{-1}$ ) but remained well below inhibitory levels for *A. niger* ( $4.04 \text{ g L}^{-1}$ ) and *P. putida* ( $6.32 \text{ g L}^{-1}$ ). As *R. toruloides* exhibits strong sensitivity to both butylamine and butylacetamide, this likely explains its inability to grow even at the lowest concentration of unfiltered hydrolysate (Fig. 1C). After charcoal treatment, the concentration of butylacetamide decreased to  $0.4 \text{ g L}^{-1}$ , and butylamine decreased to  $0.6 \text{ g L}^{-1}$ . These post-treatment concentrations were below the  $\text{IC}_{50}$  thresholds for all three organisms, demonstrating that

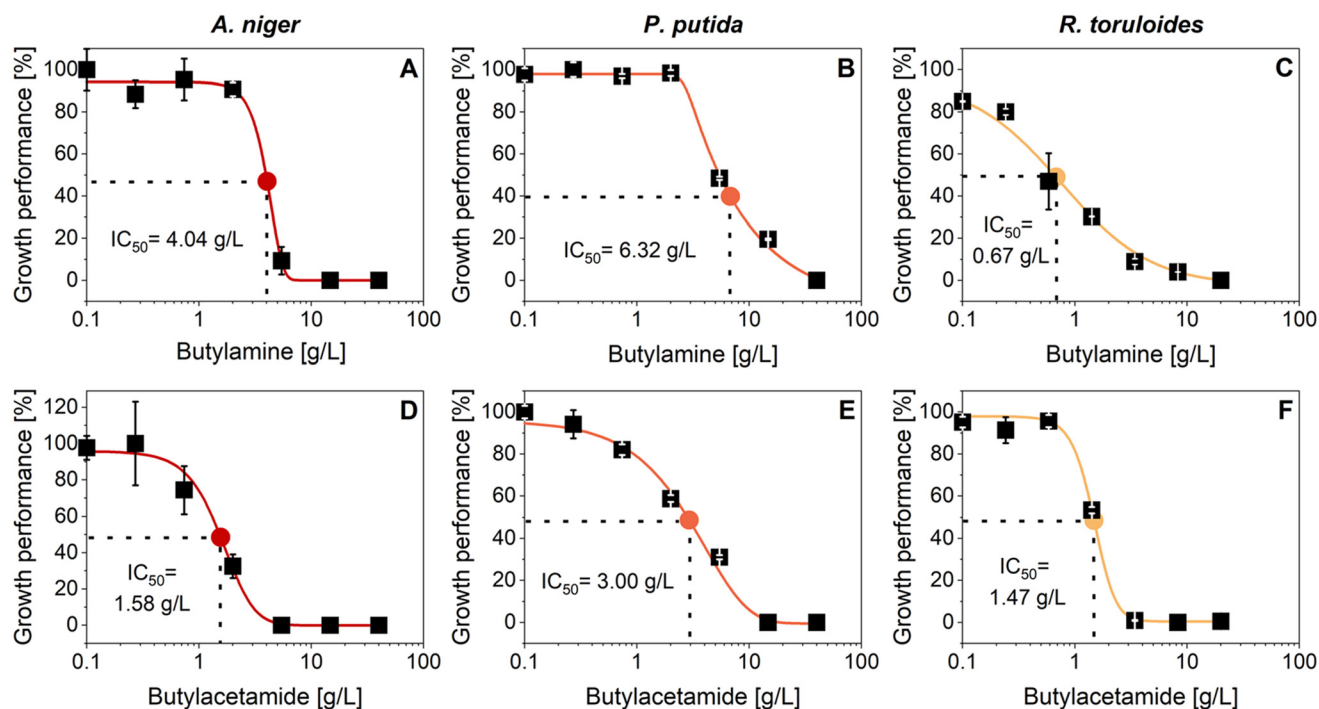


**Fig. 3**  $\text{IC}_{50}$  determination of butylamine and butylacetamide. *A. niger* (shake flask), *P. putida* and *R. toruloides* (microbioreactor plate) were grown in their respective chemically defined media with increasing concentrations of butylamine (A–C) and butylacetamide (D–F). For *A. niger*, the biomass was determined after 144 h (see Tables S2 and S3) to establish the  $\text{IC}_{50}$  whereas for *P. putida* and *R. toruloides*, the  $\text{IC}_{50}$  was determined by integration of the growth curve over 56 h (see Fig. S2). The regression model and the respective  $\text{IC}_{50}$  values were determined with a five-parameter logistic model. The data represent averages and the error bars represent standard deviations of biological triplicates (*n* = 3).



detoxification effectively mitigated chemical inhibition and improved microbial compatibility with the hydrolysate. Although we employed comprehensive analytical methods to identify and quantify known inhibitors, the chemical complexity of the hydrolysate means that we cannot fully exclude the presence of additional toxic compounds that remained undetected.

### Bioproduct accumulation with different microbial hosts

The detoxified hydrolysate was further evaluated and optimized as a cultivation medium for each of the three engineered strains. To identify species-specific limitations, nutrient supplements were added stepwise to the filtered hydrolysate. As a control, each strain was cultivated in a defined mock hydrolysate containing glucose and xylose at concentrations equivalent to the hydrolysate. The mock medium lacked the chemical complexity of biomass-derived hydrolysate enabling a direct comparison of the specific effect of nutrient availability and fermentation performance between the defined and biomass-derived media.

### Malic acid production by *Aspergillus niger*

Cultures of the malic acid producing *A. niger* strain JJ1 using mock or pure hydrolysate were supplemented sequentially with peptone (N), magnesium sulfate (Mg), monopotassium phosphate and dibasic potassium phosphate (P), and trace elements (TE;  $\text{FeSO}_4$  and  $\text{NaCl}$ ). All cultures contained  $\text{CaCO}_3$  to support pH buffering and promote organic acid accumulation.<sup>33</sup>

In the mock series, malic acid production and biomass increased progressively with nutrient addition (Fig. 4A and C). The base mock condition supported limited titers ( $6.8 \text{ g L}^{-1}$ ) and biomass ( $1.3 \text{ g L}^{-1}$ ), whereas addition of peptone drastically improved the malic acid titer ( $31.8 \text{ g L}^{-1}$ ) to 95% of the maximal titer observed in defined medium.  $\text{MgSO}_4$  as well as the addition of phosphate yielded no significant increase in malic acid or biomass production. Only the amount of sugar consumed was positively impacted by the addition of phosphate. The final addition of trace elements (Mock + N + Mg + P + TE) yielded the maximal titer achieved in defined medium, reaching  $33.4 \text{ g L}^{-1}$  malic acid and  $8.0 \text{ g L}^{-1}$  biomass. Interestingly, sugar consumption remained incomplete across all mock conditions, with particularly limited xylose utilization.

In comparison, the hydrolysate series enabled higher overall titers and biomass accumulation (Fig. 4B and D). Interestingly, the hydrolysate supported the production of  $15.6 \text{ g L}^{-1}$  of malic acid and  $5.6 \text{ g L}^{-1}$  of biomass without any supplements, suggesting that the biomass-derived matrix contains beneficial components or additional carbon sources beyond glucose and xylose. For example, it is known that amino acids in the hydrolysate can boost microbial bioproduct concentrations.<sup>34</sup> Peptone addition (Hyd + N) drastically boosted performance to  $47.0 \text{ g L}^{-1}$  malic acid and  $11.2 \text{ g L}^{-1}$  biomass, with near-complete glucose and substantial xylose consumption. Further supplementing with magnesium sulfate, monopotassium phosphate and dibasic potassium

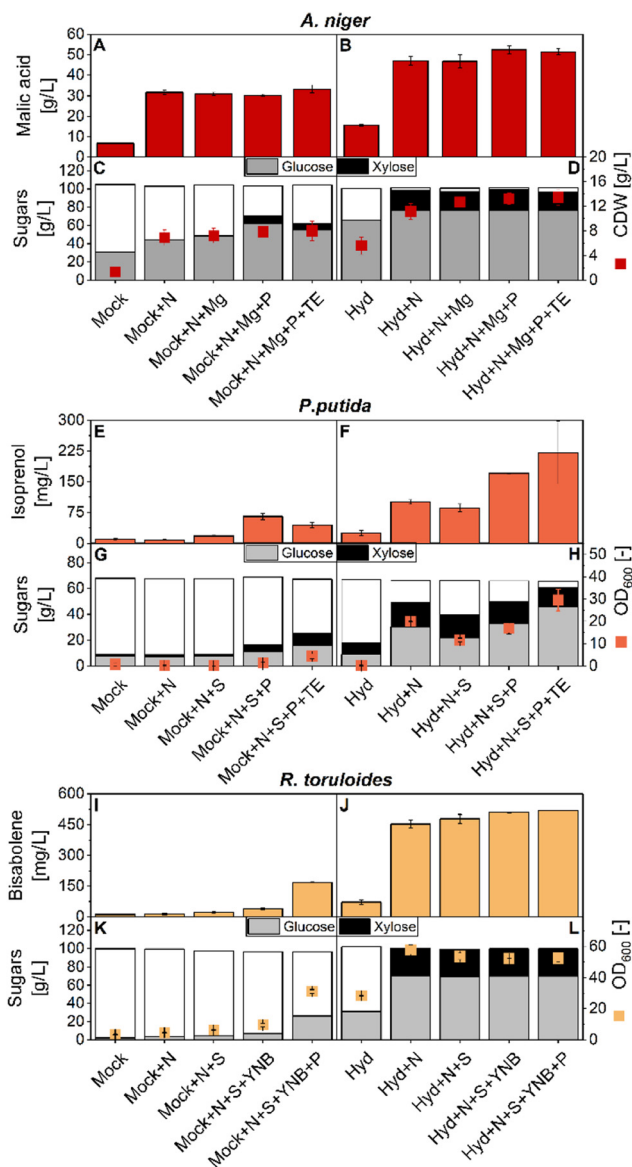


**Fig. 4** Microbial growth, sugar consumption and bioproduct accumulation in mock media containing glucose and xylose (Mock, graphs on the left) or butylamine-pretreated hydrolysate (Hyd, graphs on the right) with stepwise nutrient supplementation. Top: Malic acid production by *Aspergillus niger* after sequential addition of peptone (N), magnesium sulfate (Mg), phosphate (P), and trace elements (TE). (A and B) Malic acid titers; (C and D) sugar utilization and cell dry weight (CDW) after 144 h. Middle: Isoprenol production by *Pseudomonas putida* after sequential addition of ammonium chloride (N), sodium sulfate (S), phosphate (P), and trace elements (TE). (E and F) Isoprenol titers; (G and H) sugar utilization and final cell density ( $\text{OD}_{600}$ ) after 72 h. Bottom: Bisabolene production by *Rhodosporidium toruloides* after sequential addition of ammonium chloride (N), sodium sulfate (S), yeast nitrogen base (YNB), and phosphate (P). (I and J) Bisabolene titers; (K and L) sugar utilization and final cell density ( $\text{OD}_{600}$ ) after 144 h. White bars indicate total initial sugar concentration while grey and black bars indicate the consumed glucose and xylose amounts, respectively. Pure (100%) hydrolysate was used for *A. niger* and *R. toruloides* and hydrolysate diluted to 60% was used for *P. putida*. The data represent averages and the error bars represent standard deviations of biological triplicates ( $n = 3$ ).



phosphate, and trace elements brought titers above  $52.0 \text{ g L}^{-1}$  and biomass above  $13.0 \text{ g L}^{-1}$ , outperforming the defined medium by 53%.

The most pronounced improvement in malic acid production for both mock medium and hydrolysate was observed upon the addition of peptone, indicating that access to complex nutrients, particularly organic nitrogen sources, is a key limiting factor for *A. niger*. The modest gains achieved through supplementation with other nutrients in both the defined medium and the complex hydrolysate underscore the inherent robustness of *A. niger*, suggesting that high malic acid titers can be achieved even in nutrient-lean and therefore cost-effective formulations.

### Isoprenol production by *Pseudomonas putida*

The effect of nutrient supplementation on the substrate conversion capabilities of *P. putida* was investigated using an isoprenol-producing strain engineered to utilize xylose (IY1449SOT). The hydrolysate was diluted to 60% of its original concentration, since we found this to be optimal for *P. putida* growth and isoprenol production (see Fig. S3). The glucose and xylose concentrations in the mock media were matched to the diluted hydrolysate to serve as a defined baseline. Both media were supplemented stepwise with ammonium chloride (N), sodium sulfate (S), salts (P;  $\text{PO}_4^{3-}$  and NaCl), and trace elements (TE), based on the composition of M9 minimal medium regularly used for *P. putida*.

In the mock series, *P. putida* showed poor performance across the first three conditions (Mock, Mock + N, Mock + N + S), with  $\text{OD}_{600}$  values below 1.0, isoprenol titers under  $18 \text{ mg L}^{-1}$ , and minimal sugar consumption over 72 hours (glucose  $< 8 \text{ g L}^{-1}$ ; xylose  $< 1.5 \text{ g L}^{-1}$ ) (Fig. 4E and G). The addition of phosphate (Mock + N + S + P) improved performance considerably, with biomass reaching an  $\text{OD}_{600}$  of 1.5, along with higher sugar consumption (glucose:  $10.8 \text{ g L}^{-1}$ ; xylose:  $5.9 \text{ g L}^{-1}$  over 72 hours), and isoprenol titers ( $64.8 \text{ mg L}^{-1}$ ). Addition of trace elements (Mock + N + S + P + TE) further improved biomass yields ( $\text{OD}_{600} = 4.4$ ), while isoprenol production slightly decreased to  $44.8 \text{ mg L}^{-1}$ .

In the hydrolysate series (Fig. 4F and H), *P. putida* exhibited similarly low growth and product formation without supplementation ( $\text{OD}_{600} = 0.2$ ; isoprenol =  $25.4 \text{ mg L}^{-1}$ ). Addition of  $\text{NH}_4\text{Cl}$  (Hyd + N) improved performance, increasing the  $\text{OD}_{600}$  to 19.9 and isoprenol titers to  $100.7 \text{ mg L}^{-1}$ , alongside high sugar consumption ( $27.3 \text{ g L}^{-1}$  glucose;  $16.8 \text{ g L}^{-1}$  xylose over 72 hours). Subsequent addition of  $\text{Na}_2\text{SO}_4$  (Hyd + N + S) resulted in a slight decrease in both growth ( $\text{OD}_{600} = 11.6$ ) and isoprenol production ( $86.0 \text{ mg L}^{-1}$ ). However, further supplementation with phosphate and trace elements (Hyd + N + S + P + TE) enhanced performance, leading to the highest observed isoprenol titer of  $221.4 \text{ mg L}^{-1}$  and  $\text{OD}_{600} = 29.5$ , with over  $40 \text{ g L}^{-1}$  glucose and  $13 \text{ g L}^{-1}$  xylose consumed.

These results demonstrate that for *P. putida* the biomass-derived matrix supports substantially higher titers (3.4-fold) than a defined sugar solution. In the Hyd + N condition alone, isoprenol titers were 1.6-fold higher than those of any mock

condition, emphasizing the value of hydrolysate as a functional fermentation base once nitrogen limitation is relieved.

### Bisabolene production by *Rhodospiridium toruloides*

The nutritional potential of detoxified butylamine-pretreated poplar hydrolysate was also evaluated with a bisabolene-producing strain of *R. toruloides* grown on 100% hydrolysate and a mock medium. When using the mock, *R. toruloides* did not grow or produce bisabolene effectively on pure glucose and xylose ( $\text{OD}_{600} = 3.4$ ;  $11.4 \text{ mg L}^{-1}$ ) (Fig. 4I and K). Stepwise nutrient supplementation led to progressive increases: with  $\text{NH}_4\text{Cl}$  the growth rose to an  $\text{OD}_{600}$  of 4.4 and a bisabolene titer of  $12.7 \text{ mg L}^{-1}$ ; the addition of  $\text{Na}_2\text{SO}_4$  further improved these values ( $\text{OD}_{600} = 6.4$ ,  $21.7 \text{ mg L}^{-1}$ ). Supplementing with YNB yielded  $\text{OD}_{600} = 9.6$  and  $38.2 \text{ mg L}^{-1}$  bisabolene. The final addition of phosphate enabled the best performance in the mock series ( $\text{OD}_{600} = 31.1$ ;  $167.8 \text{ mg L}^{-1}$ ). Nevertheless, sugar consumption remained incomplete, indicating a nutrient limitation in the chemically defined media formulation.

The hydrolysate supported moderate growth ( $\text{OD}_{600} = 28.5$ ) and bisabolene production ( $77.8 \text{ mg L}^{-1}$ ), even when it was used in concentrated form and without nutrient supplementation (Fig. 4J and L). However, sugar consumption in this condition was also incomplete, suggesting limited availability of nutrients relative to the initial concentrations of sugars. Remarkably, addition of  $\text{NH}_4\text{Cl}$  (Hyd + N) led to an enhancement in both growth ( $\text{OD}_{600} = 57.9$ ) and bisabolene production ( $491.1 \text{ mg L}^{-1}$ ), accompanied by complete sugar consumption. This sole addition of  $\text{NH}_4\text{Cl}$  yielded 87% of the maximum titer observed, indicating nitrogen limitation as the primary bottleneck. Further additions of  $\text{Na}_2\text{SO}_4$ , YNB, and phosphate led to continued improvements, with final titers reaching  $562.9 \text{ mg L}^{-1}$  and sustained high biomass ( $\text{OD}_{600} = 52.5$ ), confirming that these additions further enhanced the bioconversion process.

### Comparative performance of microbial hosts in hydrolysate

The three engineered organisms used for bioconversion in this study exhibited distinct behaviors when cultivated in the hydrolysate before and after charcoal filtration. Before filtration, the hydrolysate was differentially toxic to the microbes, with *P. putida* being the most robust and *R. toruloides* being the most sensitive. As these three organisms can catabolize and tolerate many lignin-derived aromatics<sup>35–37</sup> and no furfural or 5-hydroxymethylfurfural were produced during the pretreatment reaction, the observed toxicity can be partially attributable to residual butylamine and the derivative butylacetamide. This is supported by the dose–response assays shown in Fig. 3, which consistently identified *P. putida* as the most tolerant organism, followed by *A. niger* and *R. toruloides*.

Interestingly, when the toxic compounds were removed by charcoal filtration, *P. putida* was the only organism that reached maximum cell density, substrate consumption and product accumulation at 60% hydrolysate concentration, while the other microbes did so at 100% hydrolysate concentration. This indicates that other process configurations such as fed-



batch could be explored to maintain sugar concentrations under a certain threshold and avoid growth inhibition due to osmotic pressure, which is known to primarily affect bacteria like *P. putida*.<sup>38</sup>

Although charcoal filtration is widely used industrially and can be implemented at scale,<sup>39</sup> it may also be possible to minimize hydrolysate toxicity by adjusting the reaction conditions used during biomass pretreatment and solvent removal. For example, the use of milder reaction conditions could prevent or reduce the occurrence of amidation reactions responsible for butylacetamide formation. Likewise, high solvent removal yields (>98%) have been reported at smaller reactor scales and when using other amine-functionalized solvents and removal methods.<sup>16,40</sup> The inclusion of distillation or other solvent recovery techniques could increase the removal of butylamine, potentially improving the biocompatibility of the hydrolysate and allowing for solvent reuse.

Overall, the poplar hydrolysates generated in this work supported microbial growth after charcoal treatment and all strains required only supplementation with a nitrogen source to achieve higher growth and bioproduct titers compared to hydrolysates without supplementation. The ability to valorize high concentrations of sugars in amine-pretreated hydrolysates using microbial fermentation provides an important alternative over current approaches by combining simple solvent evaporation and hydrolysate conditioning methods with the use of engineered strains that allow for the accumulation of diverse bioproducts and enable further process intensification strategies.

*A. niger* stood out for its ability to produce high levels of malic acid (up to 52 g L<sup>-1</sup>), particularly in the presence of peptone and inorganic salts, underscoring its value as fungal chassis for organic acid biosynthesis from lignocellulosic feedstocks. Notably, it responded positively to the hydrolysate matrix even without supplementation, suggesting some endogenous capacity for nutrient scavenging. *P. putida* showed the highest tolerance to residual inhibitors, achieving substantial growth (OD<sub>600</sub> > 20) and product formation (>100 mg L<sup>-1</sup>) with simple NH<sub>4</sub>Cl supplementation. Its ability to rapidly consume both glucose and xylose, combined with its robust stress response systems, makes it a promising candidate for direct fermentation of butylamine-treated biomass hydrolysates. *R. toruloides* produced similar cell densities and bisabolene titers when the hydrolysates were supplied with only NH<sub>4</sub>Cl, compared to the fully supplemented hydrolysates. The detoxified and supplemented hydrolysates enabled high-density growth (up to OD<sub>600</sub> = 52) and complete conversion of sugars with relatively simple nutrient additions. These traits reinforce *R. toruloides* as an attractive host for terpene production in nutrient-adjusted lignocellulosic media.

## Conclusions

Our findings showcase butylamine-treated poplar hydrolysate as a robust and chemically rich feedstock, requiring only sup-

plementation with NH<sub>4</sub>Cl to match or exceed bioproduct titers achievable in defined media. The deconstruction process resulted in high sugar concentrations, saccharification yields and solvent recovery efficiency; however, the hydrolysates contained butylamine and butylacetamide at sufficiently high concentrations to exert toxicity on the microbial hosts. Performing charcoal treatment of the hydrolysate significantly improved the compatibility with all organisms, enabling them to assimilate up to 100 g L<sup>-1</sup> of sugars in batch mode. This difference in process performance highlights the importance of carefully identifying the pretreatment solvent and reaction conditions that not only maximize sugar release but also minimize the formation of toxic compounds like amides. Importantly, the detoxified hydrolysate successfully supported diverse microbial platforms, demonstrating the versatility of the process and its potential for broad application across different fermentation systems.

## Experimental

### Chemicals and plant biomass feedstock

All chemicals were purchased from Sigma-Aldrich if not otherwise stated (Sigma-Aldrich, St Louis, MO, USA). Hybrid poplar (*Populus alba* × *grandidentata*) was used as the lignocellulosic feedstock. Trees were greenhouse-grown under previously described conditions.<sup>41</sup> The biomass was first reduced to mulch using a commercial woodchipper, milled in a knife mill (model 4, Thomas Scientific, Swedesboro, NJ, USA), and sieved to a uniform particle size of 2 mm to ensure consistency prior to pretreatment.

### Biomass pretreatment

Pretreatment was carried out by mixing poplar biomass at a solid loading of 15 wt% with neat *n*-butylamine (hereafter referred to as butylamine) (85 wt%) using a reaction volume of 3 L in a 10 L reactor (4555-58, Parr Instruments Company, Moline, IL, USA) and heating at 140 °C for 3 h. Due to the scale of the reaction, a single pretreatment run was performed. Post pretreatment, the vessel was cooled down to room temperature and the pretreated mixture was transferred into a Teflon tray. The pretreated sample was then dried at 80 °C under house vacuum for 12 h. The residual dry biomass weight was used to determine the amount of solvent removed by evaporation.

### Enzymatic hydrolysis and hydrolysate conditioning

Enzymatic hydrolysis of dried biomass was carried out after adjusting the pH to 5 by adding water and 72% sulfuric acid, followed by the addition of the commercial cellulase and hemicellulase cocktails Cellic® CTec3 and HTec3 (Novozymes, Franklinton, NC, USA). The CTec3 and HTec3 cocktails were first mixed at a 9 : 1 (v/v) ratio and added at a final concentration of 30 mg enzyme per g of biomass in a 500 mL glass bottle to carry out saccharification at 50 °C for 72 h in an incubator with rotating platform (Thermo Fisher Scientific,



Waltham, MA, USA). The hydrolysate was separated from the lignin-rich solid fraction and filtered with a 0.45  $\mu\text{m}$  Nalgene® filter (Thermo Fisher Scientific, Waltham, MA, USA). The hydrolysate was then mixed with 1/10<sup>th</sup> volume of 40–60 mesh charcoal (Fluka, USA) and sonicated for 10 minutes. The charcoal was allowed to settle down at room temperature, and the supernatant was passed through 0.2  $\mu\text{m}$  Nalgene® filters (Thermo Fisher Scientific, Waltham, MA, USA).

### Microbial strains

The strains and plasmid sequences used in this work are deposited in the Joint BioEnergy Institute public registry and can be accessed at <https://public-registry.jbei.org> with the following ID numbers (in parentheses): *A. niger* JJ1 (JBx\_275419), *R. toruloides* GB2 (ABFPUB\_000311), and *P. putida* IY1449SOT (JBx\_257853). A list of strain genotypes and features is provided in Table S4. *A. niger* JJ1 was engineered to produce malic acid by transforming a C4-dicarboxylate transporter gene from *Aspergillus oryzae*, that is codon-optimized and controlled by the *gpdA* promoter from *A. niger*.<sup>42</sup> *R. toruloides* GB2 was previously engineered to produce  $\alpha$ -bisabolene by performing genome integration of multiple copies of a heterologous bisabolene synthase enzyme.<sup>43</sup> *P. putida* IY1449SOT was engineered for isoprenol production through seven targeted gene knockouts guided by genome-scale metabolic modeling, combined with optimization of the IPP-bypass and xylose pathway.

### Microbial growth comparisons in hydrolysates

The toxicity of the hydrolysate from enzymatic hydrolysis of butylamine-pretreated poplar was assessed by evaluating its effects on microbial growth. For *A. niger*, complete medium (CM) was used as the diluent. CM was prepared according to a previously described method.<sup>44</sup> For *P. putida*, hydrolysate was diluted in LB medium, while for *R. toruloides*, YPD medium was used as the diluent. CM, LB, and YPD media without hydrolysate were used as controls.

*A. niger* strains were maintained on CM agar plate at 30 °C for spore preparation. Spores were harvested by washing with 5–10 mL sterile 0.4% Tween 80 (polyoxyethylene-sorbitan monooleate). Approximately  $1 \times 10^8$  spores of *A. niger* were added to CM in a 250 mL Erlenmeyer flask. The cultures were grown overnight at 30 °C at 200 rpm. The mycelia were harvested by filtering the culture through Miracloth and rinsed with sterile water. Mycelia were transferred into CM in 250 mL Erlenmeyer flask, and the cultures were incubated at 30 °C, 200 rpm for 3 days. Mycelial dry cell weight was determined by harvesting the mycelia on a pre-weighed filter by vacuum filtration and washing with distilled water. Subsequently, the dry weight was determined after freeze-drying in a lyophilizer. *P. putida* and *R. toruloides* cells from a single colony were grown overnight in LB and YPD medium at 200 rpm and 30 °C. Overnight cultures were used to inoculate a culture medium in 24-well plates (Costar, Corning, NY, USA) with a working volume of 1 mL and at a starting optical density  $\text{OD}_{600} = 0.1$ . Cultures were incubated at 30 °C at 200 rpm for 3 days.

### Butylamine and butylacetamide toxicity assays

Each organism was exposed to a log-spaced series of butylamine and butylacetamide concentrations (Table S5) to assess compound toxicity. Concentrations were selected to span sub-inhibitory to fully inhibitory levels, enabling robust curve fitting for each species. Toxicity assays for *A. niger* were performed in 250 mL Erlenmeyer flasks containing CM inoculated with  $1 \times 10^8$  spores, pre-cultured overnight, and transferred to chemically defined medium for 7 days at 30 °C and 200 rpm. Growth performance was determined by endpoint dry cell weight and normalized to the control condition (0 g L<sup>-1</sup> butylamine or butylacetamide). The chemically defined medium for *A. niger* grow containing 67 g L<sup>-1</sup> glucose, 33 g L<sup>-1</sup> xylose, 6 g L<sup>-1</sup> Bacto peptone, 0.10 g L<sup>-1</sup> of MgSO<sub>4</sub>·7H<sub>2</sub>O, 0.15 g L<sup>-1</sup> KH<sub>2</sub>PO<sub>4</sub>, 0.15 g L<sup>-1</sup> K<sub>2</sub>HPO<sub>4</sub>, 0.10 g L<sup>-1</sup> CaCl<sub>2</sub>·2H<sub>2</sub>O, 0.005 g L<sup>-1</sup> of FeSO<sub>4</sub>·7H<sub>2</sub>O, and 0.005 g L<sup>-1</sup> of NaCl. Toxicity assays for *P. putida* and *R. toruloides* were performed in 48-well FlowerPlates (M2P-48-B, m2p-labs, Islandia, NY, USA) using a microbioreactor system (BioLector II Pro, m2p-labs, Baesweiler, Germany). Cultures were grown in a chemically defined medium, with each condition tested in triplicate. Biomass accumulation was monitored by online light scattering at 620 nm. Growth performance was quantified by integrating the growth curves up to 56 h, and the resulting area under the curve (AUC) values were normalized to the control condition (0 g L<sup>-1</sup> butylamine or butylacetamide). *P. putida* was cultivated in medium containing 67 g L<sup>-1</sup> glucose, 33 g L<sup>-1</sup> xylose, 10 g L<sup>-1</sup> NH<sub>4</sub>Cl, 10 g L<sup>-1</sup> Na<sub>2</sub>SO<sub>4</sub>, 1 $\times$  M9 salts, 4 mM MgSO<sub>4</sub>, 0.2 mM CaCl<sub>2</sub>, and 1 $\times$  trace metal solution (Teknova, Hollister, CA, USA). *R. toruloides* was grown in medium containing 67 g L<sup>-1</sup> glucose, 33 g L<sup>-1</sup> xylose, 1.7 g L<sup>-1</sup> yeast nitrogen base (YNB; w/o AA and (NH<sub>4</sub>)<sub>2</sub>SO<sub>4</sub>), 5 g L<sup>-1</sup> NH<sub>4</sub>Cl, 5 g L<sup>-1</sup> Na<sub>2</sub>SO<sub>4</sub>, and 100 mM phosphate buffer (pH 6.2).

The half-maximal inhibitory concentration (IC<sub>50</sub>) values for butylamine and butylacetamide for each organism were determined using a five-parameter logistic regression model. Compounds were tested across a range of concentrations as listed in Table S3.

### Bioproduct accumulation campaigns

*A. niger* spores were harvested by washing with 5–10 mL sterile 0.4% Tween 80. Approximately  $1 \times 10^8$  spores were used to inoculate. For malic acid production experiments, the butylamine-pretreated hydrolysate was supplemented with a stepwise combination of defined nutrients depending on the experimental condition. Supplements included 80.00 g L<sup>-1</sup> of CaCO<sub>3</sub>, 6 g L<sup>-1</sup> Bacto peptone, 0.10 g L<sup>-1</sup> of MgSO<sub>4</sub>·7H<sub>2</sub>O, 0.15 g L<sup>-1</sup> KH<sub>2</sub>PO<sub>4</sub>, 0.15 g L<sup>-1</sup> K<sub>2</sub>HPO<sub>4</sub>, 0.10 g L<sup>-1</sup> CaCl<sub>2</sub>·2H<sub>2</sub>O, 0.005 g L<sup>-1</sup> of FeSO<sub>4</sub>·7H<sub>2</sub>O, and 0.005 g L<sup>-1</sup> of NaCl. Sugar-matched mock media (70 g L<sup>-1</sup> glucose, 30 g L<sup>-1</sup> xylose) were prepared and supplemented in parallel with the same combinations to serve as controls for direct comparison. The malic acid production experiments were conducted in a 125 mL Erlenmeyer flask and incubated at 30 °C, 200 rpm in a plat-



form shaker (INFORS HT Multitron 2, Annapolis Junction, MD, USA).

A single colony of *P. putida* was inoculated into 1 mL LB medium containing kanamycin ( $50 \mu\text{g mL}^{-1}$ ) and cultivated overnight at  $30^\circ\text{C}$ , 1000 rpm and 80% humidity in a platform shaker (INFORS HT Multitron 4, Annapolis Junction, MD, USA). The overnight culture was used to inoculate M9-NREL medium to an initial  $\text{OD}_{600}$  of 0.1. The M9-NREL medium contained  $10 \text{ g L}^{-1}$  glucose,  $10 \text{ g L}^{-1}$  xylose,  $1\times$  M9 salts,  $2 \text{ mM MgSO}_4$ ,  $0.1 \text{ mM CaCl}_2$ ,  $1\times$  trace metal solution (Teknova, Hollister, CA, USA), and  $5 \text{ g L}^{-1}$   $(\text{NH}_4)_2\text{SO}_4$ . For isoprenol production experiments, the butylamine-pretreated hydrolysate was diluted to 60% (v/v) and supplemented with a stepwise combination of defined nutrients depending on the experimental condition. Supplements included  $10 \text{ g L}^{-1}$   $\text{NH}_4\text{Cl}$ ,  $10 \text{ g L}^{-1}$   $\text{Na}_2\text{SO}_4$ ,  $1\times$  M9 salts,  $4 \text{ mM MgSO}_4$ ,  $0.2 \text{ mM CaCl}_2$ , and  $1\times$  trace metal solution (Teknova). Sugar-matched mock media ( $42 \text{ g L}^{-1}$  glucose,  $18 \text{ g L}^{-1}$  xylose) were prepared and supplemented in parallel with the same combinations to serve as controls for direct comparison. A pentadecane overlay (20% of the culture volume) was added to capture the product. The isoprenol production experiments were conducted in 48-well flower plates (M2P-48-B, m2p-labs, Islandia, NY, USA) sealed with an Aeraseal air-permeable seal (Excel Scientific, Victorville, CA, USA) at  $30^\circ\text{C}$ , 1000 rpm and 80% humidity.

*R. toruloides* precultures were inoculated from a cryo stock into chemically defined media containing  $1.7 \text{ g L}^{-1}$  YNB,  $35 \text{ g L}^{-1}$  glucose,  $15 \text{ g L}^{-1}$  xylose,  $5 \text{ g L}^{-1}$   $(\text{NH}_4)_2\text{SO}_4$  and  $100 \text{ mM}$  phosphate buffer ( $\text{pH} = 6.2$ ), and grown overnight at  $30^\circ\text{C}$ , 1000 rpm and 80% humidity in a platform shaker (INFORS HT Multitron 4, Annapolis Junction, MD, USA). For bisabolene production experiments, the butylamine-pretreated hydrolysate was supplemented with a stepwise combination of defined nutrients depending on the experimental condition. Supplements included  $1.7 \text{ g L}^{-1}$  YNB,  $5 \text{ g L}^{-1}$   $\text{NH}_4\text{Cl}$ , and  $5 \text{ g L}^{-1}$   $\text{Na}_2\text{SO}_4$ , and  $100 \text{ mM}$  phosphate buffer ( $\text{pH} = 6.2$ ). Sugar-matched mock media ( $70 \text{ g L}^{-1}$  glucose,  $30 \text{ g L}^{-1}$  xylose) were prepared and supplemented in parallel with the same combinations to serve as controls for direct comparison. A pentadecane overlay (20% of the culture volume) was added to capture bisabolene. Each condition was inoculated from the preculture with an initial  $\text{OD}_{600}$  of 0.1. The production experiments were conducted in 48-well flower plates (M2P-48-B, m2p-labs, Islandia, NY, USA) sealed with an Aeraseal air-permeable seal (Excel Scientific, Victorville, CA, USA) at  $30^\circ\text{C}$ , 1000 rpm and 80% humidity.

### Analytical methods

For sugar analysis, samples were filtered through  $0.45 \mu\text{m}$  polypropylene filter plate (Agilent, Santa Clara, CA, USA) and  $5 \mu\text{L}$  sample injection volumes were used. Glucose and xylose were quantified with an Agilent Technologies 1200 series HPLC system equipped with an Aminex HPX-87H column (BioRad Laboratories, Hercules, CA, USA), with refractive index detector, kept at  $60^\circ\text{C}$  during analysis.  $4 \text{ mM}$  sulfuric acid was used as a mobile phase with a flow rate of  $0.6 \text{ mL min}^{-1}$ .

Phenolic compounds were analyzed using a previously described method.<sup>45</sup> Butylamine and associated amides were separated on a Kinetex Phenyl-hexyl column (with an internal diameter of  $4.6 \text{ mm}$ , column length of  $100 \text{ mm}$ , and stationary phase particle size of  $2.6 \mu\text{m}$  from Phenomenex, Torrance, CA, USA) via an Agilent Technologies 1260 Infinity HPLC system. The HPLC sample tray, column compartment, and injection volume were set to  $6^\circ\text{C}$ ,  $50^\circ\text{C}$ , and  $1 \mu\text{L}$ , respectively. HPLC solvents A and B were  $0.4\%$  formic acid ( $98\% \geq$  chemical purity from Sigma-Aldrich, St Louis, MO, USA) in LC-MS grade water (Honeywell Burdick & Jackson, Charlotte, NC, USA) and  $0.4\%$  formic acid in LC-MS grade methanol (Honeywell Burdick & Jackson, Charlotte, NC, USA), respectively. Gradient elution was conducted as follows: linearly increased from 5% solvent B to 25% B in 2.0 min, increased from 25% B to 90% B in 1.0 min, held at 90% B for 4.5 min, linearly decreased from 90% B to 5% B in 0.3 min, and held at 5% B for 2 min. The flow rate was held at  $0.6 \text{ mL min}^{-1}$  for 7.5 min, increased from  $0.6 \text{ mL min}^{-1}$  to  $1.0 \text{ mL min}^{-1}$  in 0.3 min, and held at  $1.0 \text{ mL min}^{-1}$  for 2 min. The total LC run time was 9.8 min. The HPLC system was coupled to an Agilent Technologies 6520 quadrupole time-of-flight mass spectrometer. For electrospray ionization (ESI), drying and nebulizer gases were set to  $11 \text{ L min}^{-1}$  and 30 psi, respectively, and a drying gas temperature of  $340^\circ\text{C}$  was used throughout. ESI was conducted in the negative ion mode with a capillary voltage of 3500 V. The fragmentor, skimmer, and OCT 1 RF  $V_{\text{pp}}$  voltages were set to 100 V, 60 V, and 400 V, respectively. Data acquisition was performed via Agilent Technologies MassHunter Workstation (version 8) and data analysis by MassHunter Qualitative Analysis (version 6), Profinder (version 8), and MassHunter Quantitative Analysis (version 10). Analytes were quantified by external calibration curves.

Malic acid concentrations were quantified with an Agilent Technologies 1200 series HPLC system equipped with an Aminex HPX-87H column (BioRad Laboratories, Hercules, CA, USA), with Deuterium lamp for diode array detectors collecting signal at 210 nm, kept at  $50^\circ\text{C}$  during analysis.  $4 \text{ mM}$  sulfuric acid was used as a mobile phase with a flow rate of  $0.55 \text{ mL min}^{-1}$ . Prior to analysis, samples were filtered through  $0.45 \mu\text{m}$  polypropylene filter plate (Agilent, Santa Clara, CA, USA) and  $5 \mu\text{L}$  sample injection volumes were used.

Bisabolene concentrations were quantified by mixing a  $2 \mu\text{L}$  aliquot from the pentadecane overlay with  $48 \mu\text{L}$  of ethyl acetate containing hexadecane ( $50 \text{ mg L}^{-1}$ ) as an internal standard. Samples ( $1 \mu\text{L}$ ) were analyzed by GC-MS (7890A GC; 5975C MS; Agilent, Santa Clara, CA, USA) using a HP-5MS column ( $30 \text{ m} \times 0.25 \text{ mm i.d.}$ ,  $0.25 \mu\text{m}$  film thickness; Agilent, Santa Clara, CA, USA) The GC oven temperature program was as follows: hold  $70^\circ\text{C}$  for 1 min then  $70^\circ\text{C}$  to  $220^\circ\text{C}$  at  $30^\circ\text{C min}^{-1}$ , followed by a 2 min hold at  $220^\circ\text{C}$ . The inlet temperature was set to  $200^\circ\text{C}$ . Final titers were back-calculated from the overlay to the aqueous phase to reflect the concentration in the culture medium.

Isoprenol concentrations were quantified from *P. putida* cultures using a 20% pentadecane overlay. Cultures were centrifuged at  $18\ 000g$  to separate the organic and aqueous phases.



A 10  $\mu\text{L}$  aliquot of the pentadecane overlay was diluted in 990  $\mu\text{L}$  ethyl acetate containing 1-butanol (30  $\text{mg L}^{-1}$ ) as an internal standard. Samples (1  $\mu\text{L}$ ) were analyzed by gas chromatography with flame ionization detection (GC-FID; Thermo Focus GC, Thermo Fisher Scientific, Waltham, MA, USA) using a DB-WAX column (15  $\text{m} \times 0.32$  mm i.d., 0.25  $\mu\text{m}$  film thickness; Agilent, Santa Clara, CA, USA). The GC oven temperature program was as follows: 40  $^{\circ}\text{C}$  to 100  $^{\circ}\text{C}$  at 15  $^{\circ}\text{C min}^{-1}$ , then to 230  $^{\circ}\text{C}$  at 40  $^{\circ}\text{C min}^{-1}$ , followed by a 2 min hold at 230  $^{\circ}\text{C}$ . The inlet temperature was set to 200  $^{\circ}\text{C}$ . Final titers were back-calculated from the overlay to the aqueous phase to reflect the concentration in the culture medium. Calibration curves were built for all quantified compounds using linear regression and used to determine the concentration in the analyzed samples.

### Quantification and statistical analysis

Statistical analysis was performed using OriginPro 2025 (OriginLab, Northampton, MA, USA). Each experiment was performed in technical triplicates (derived from the same preculture) unless otherwise stated. Error bars represent the standard deviation from the mean, as indicated by  $\pm$  in the tables and figures. For toxicity assays,  $\text{IC}_{50}$  values were determined using non-linear curve fitting with a five-parameter logistic regression model in OriginPro 2025.

## Author contributions

Conceptualization: J. J., D. D., J. P., B. A. S., J. K., A. R.; data curation: J. J., D. D., V. R. P., E. A. T., E. E. K. B., C. A. B., M. M. R.; formal analysis: J. J., D. D., V. R. P., E. A. T., E. E. K. B., C. A. B., M. M. R., E. K., J. P.; funding acquisition: B. A. S.; investigation: J. J., D. D., V. R. P., E. A. T., E. K., J. P.; methodology: E. E. K. B., C. W. K., V. E. G., E. R. S., A. E., H. C., T. S. L., J. K.; project administration: B. A. S., J. K., A. R.; resources: J. P., C. W. K., V. E. G., E. R. S., A. E., H. C., T. S. L., J. M. G.; supervision: E. R. S., H. C., J. M. G., B. A. S., J. K., A. R.; writing – original draft: J. J., D. D.; writing – review & editing: J. J., D. D., J. K., V. E. G., A. R.

## Conflicts of interest

B. A. S. has a financial interest in Illium Technologies, Caribou Biofuels, and Erg Bio. All other authors declare the absence of any commercial or financial relationships that could be construed as a potential conflict of interest.

## Data availability

The data supporting this article have been included as part of the supplementary information (SI). Supplementary information is available. See DOI: <https://doi.org/10.1039/d5gc06335c>.

## Acknowledgements

The work conducted at the Joint BioEnergy Institute was supported by the U.S. Department of Energy, Office of Science, Biological and Environmental Research Program, through contract DE-AC02-05CH11231 between Lawrence Berkeley National Laboratory and the U.S. Department of Energy. The United States Government retains and the publisher, by accepting the article for publication, acknowledges that the United States Government retains a non-exclusive, paid-up, irrevocable, worldwide license to publish or reproduce the published form of this manuscript, or allow others to do so, for United States Government purposes. Any subjective views or opinions that might be expressed in this paper do not necessarily represent the views of the U.S. Department of Energy or the United States Government. Sandia National Laboratories is a multi-mission laboratory managed and operated by National Technology & Engineering Solutions of Sandia, LLC, a wholly owned subsidiary of Honeywell International Inc., for the U.S. Department of Energy's National Nuclear Security Administration under contract DE-NA0003525. Pacific Northwest National Laboratory is operated for the U.S. Department of Energy by Battelle under contract DE-AC05-76RL01830. The graphical abstract was created in BioRender. Dietrich, D. (2025) <https://BioRender.com/0cxploj>.

## References

- 1 M. H. Langholtz, C. Brandt, R. Clark, H. Cook, S. Curran, M. Davis, D. De La Torre Ugarte, R. Efrogmson, J. Field and C. Hellwinckel, *2023 Billion-Ton Report: An Assessment of U.S. Renewable Carbon Resources*, 2024, DOI: [10.2172/2441098](https://doi.org/10.2172/2441098).
- 2 Y. M. Bar-On, R. Phillips and R. Milo, *Proc. Natl. Acad. Sci. U. S. A.*, 2018, **115**, 6506–6511.
- 3 B. Segers, P. Nimmegeers, M. Spiller, G. Tofani, E. Jasiukaitytė-Grozddek, E. Dace, T. Kikas, J. M. Marchetti, M. Rajić and G. Yildiz, *RSC Sustainability*, 2024, **2**, 3730–3749.
- 4 K. Ding, D. Liu, X. Chen, H. Zhang, S. Shi, X. Guo, L. Zhou, L. Han and W. Xiao, *Renewable Sustainable Energy Rev.*, 2024, **202**, 114692.
- 5 B. Long, F. Zhang, S. Y. Dai, M. Foston, Y. J. Tang and J. S. Yuan, *Nat. Rev. Bioeng.*, 2025, **3**, 230–244.
- 6 D. B. Sulis, N. Lavoine, H. Sederoff, X. Jiang, B. M. Marques, K. Lan, C. Cofre-Vega, R. Barrangou and J. P. Wang, *Nat. Commun.*, 2025, **16**, 1244.
- 7 A. P. Ingle, S. Saxena, M. P. Moharil, J. D. Rivaldi, L. Ramos and A. K. Chandel, *Biotechnol. Sustainable Mater.*, 2025, **2**, 3.
- 8 A. Woźniak, K. Kuligowski, L. Świerczek and A. Cenian, *Sustainability*, 2025, **17**, 287.
- 9 A. S. Bharadwaj, S. Dev, J. Zhuang, Y. Wang, C. G. Yoo, B.-H. Jeon, S. Aggarwal, S. H. Park and T. H. Kim, *Bioresour. Technol.*, 2023, **368**, 128339.
- 10 R. Zhai, J. Hu and M. Jin, *Biotechnol. Adv.*, 2022, **61**, 108044.



- 11 K. H. Kim and C. G. Yoo, *Front. Chem. Eng.*, 2021, **3**, 785709.
- 12 N. I. Haykir and J. Viell, *Ind. Eng. Chem. Res.*, 2024, **63**, 12251–12264.
- 13 S. Ntakirutimana, T. Xu, H. Liu, J.-Q. Cui, Q.-J. Zong, Z.-H. Liu, B.-Z. Li and Y.-J. Yuan, *Green Chem.*, 2022, **24**, 5460–5478.
- 14 M. Tanaka, G.-J. Song, R. Matsuno and T. Kamikubo, *Appl. Microbiol. Biotechnol.*, 1985, **22**, 19–25.
- 15 M. Tanaka, G.-J. Song, R. Matsuno and T. Kamikubo, *Appl. Microbiol. Biotechnol.*, 1985, **22**, 13–18.
- 16 X. Chen, A. Krishnamoorthy, J. Palasz, V. R. Pidatala, T. Lewis, Y. Tian, C. Barcelos, X. Zhou, X. Kang and Y. Han, *Biofuel Res. J.*, 2025, **12**, 2487–2502.
- 17 J. M. Palasz, A. Krishnamoorthy, R. A. Giovine, X. Chen, V. Pidatala, E. A. Turumtay, T. S. A. Lewis, E. E. K. Baidoo, C. Dou, H. Choudhary, N. Sun and B. A. Simmons, *Green Chem.*, 2025, **27**, 10117–10131.
- 18 K.-T. Hsin, H. Lee, Y.-C. Huang, G.-J. Lin, P.-Y. Lin, Y.-C. J. Lin and P.-Y. Chen, *Front. Microbiol.*, 2025, **16**, 1583746.
- 19 O. B. Chukwuma, M. Rafatullah, H. A. Tajarudin and N. Ismail, *Int. J. Environ. Res. Public Health*, 2021, **18**, 6001.
- 20 J. Detain and L. Besaury, *Curr. Res. Microb. Sci.*, 2024, **7**, 100271.
- 21 Q. Xu, W. Wang, Y. Chen, C. Zhang and N. Wu, *Ind. Crops Prod.*, 2025, **226**, 120736.
- 22 D. Banerjee, I. S. Yunus, X. Wang, J. Kim, A. Srinivasan, R. Menchavez, Y. Chen, J. W. Gin, C. J. Petzold and H. G. Martin, *Metab. Eng.*, 2024, **82**, 157–170.
- 23 G. M. de Siqueira, A. Srinivasan, Y. Chen, J. W. Gin, C. J. Petzold, T. S. Lee, M.-E. Guazzaroni, T. Eng and A. Mukhopadhyay, *Appl. Environ. Microbiol.*, 2025, **91**, e02123–e02124.
- 24 A. Rodriguez, N. Ersig, G. M. Geiselman, K. Seibel, B. A. Simmons, J. K. Magnuson, A. Eudes and J. M. Gladden, *Bioresour. Technol.*, 2019, **286**, 121365.
- 25 A. K. Chandel, S. S. Da Silva and O. V. Singh, *Bioenergy Res.*, 2013, **6**, 388–401.
- 26 V. C. Ujor and C. C. Okonkwo, *Front. Bioeng. Biotechnol.*, 2022, **10**, 1061667.
- 27 Y. An, Y. Liu, Y. Liu, M. Lu, X. Kang, S. D. Mansfield, W. Zeng and J. Zhang, *GCB Bioenergy*, 2021, **13**, 905–913.
- 28 E. C. van der Pol, R. R. Bakker, P. Baets and G. Eggink, *Appl. Microbiol. Biotechnol.*, 2014, **98**, 9579–9593.
- 29 F. Campos, J. Couto, A. Figueiredo, I. Tóth, A. O. Rangel and T. Hogg, *Int. J. Food Microbiol.*, 2009, **135**, 144–151.
- 30 A. P. Tavares, M. J. Gonçalves, T. Brás, G. R. Pesce, A. M. Xavier and M. C. Fernandes, *Energies*, 2022, **15**, 1993.
- 31 H. Miyafuji, H. Danner, M. Neureiter, C. Thomasser, J. Bvochora, O. Szolar and R. Braun, *Enzyme Microb. Technol.*, 2003, **32**, 396–400.
- 32 J. Zhao, S. Ou, S. Ding, Y. Wang and Y. Wang, *Chem. Eng. Res. Des.*, 2011, **89**, 2176–2181.
- 33 S. H. Brown, L. Bashkirova, R. Berka, T. Chandler, T. Doty, K. McCall, M. McCulloch, S. McFarland, S. Thompson and D. Yaver, *Appl. Microbiol. Biotechnol.*, 2013, **97**, 8903–8912.
- 34 J. Dong, Y. Chen, V. T. Benites, E. E. K. Baidoo, C. J. Petzold, H. R. Beller, A. Eudes, H. V. Scheller, P. D. Adams, A. Mukhopadhyay, B. A. Simmons and S. W. Singer, *Biotechnol. Bioeng.*, 2019, **116**, 1909–1922.
- 35 J. Yaegashi, J. Kirby, M. Ito, J. Sun, T. Dutta, M. Mirsiaghi, E. R. Sundstrom, A. Rodriguez, E. Baidoo and D. Tanjore, *Biotechnol. Biofuels*, 2017, **10**, 241.
- 36 R. J. Lubbers, *Microorganisms*, 2025, **13**, 1718.
- 37 R. A. Wilkes, A. J. Borchert, V. E. Garcia, G. M. Geiselman, S. Liu, A. M. Guss, J. K. Michener, D. R. Noguera, E. Masai and J. M. Gladden, *Green Chem.*, 2024, **26**, 12053–12069.
- 38 Z. Sun, J. A. Ramsay, M. Guay and B. A. Ramsay, *Appl. Microbiol. Biotechnol.*, 2006, **71**, 423–431.
- 39 R. Gupta, G. Mehta and R. C. Kuhad, *J. Chem. Technol. Biotechnol.*, 2016, **91**, 1826–1834.
- 40 E. C. Achinivu, B. W. Blankenship, N. R. Baral, H. Choudhary, R. Kakumanu, M. Mohan, E. E. Baidoo, C. D. Scown, A. George and B. A. Simmons, *Chem. Eng. J.*, 2024, **479**, 147824.
- 41 C.-Y. Lin, G. M. Geiselman, D. Liu, H. D. Magurudeniya, A. Rodriguez, Y.-C. Chen, V. Pidatala, F. Unda, B. Amer and E. E. Baidoo, *Biotechnol. Biofuels Bioprod.*, 2022, **15**, 145.
- 42 J. Jia, Z. Dai, Y. Han, H. Choudhary, G. Yuan, J. M. Gladden, B. A. Simmons, S. E. Baker, J. K. Magnuson and J. Kim, *Bioresour. Technol.*, 2026, 134018.
- 43 J. Kirby, G. M. Geiselman, J. Yaegashi, J. Kim, X. Zhuang, M. B. Tran-Gyamfi, J.-P. Prah, E. R. Sundstrom, Y. Gao and N. Munoz, *Biotechnol. Biofuels*, 2021, **14**, 101.
- 44 J. Bennett and L. Lasure, *More gene manipulations in fungi*, Academic Press, 1991, pp. 441–447.
- 45 B. Amer, R. Kakumanu, Y. Tian, A. Eudes and E. Ek Baidoo, 2021, *Targeted analysis of phenolic compounds by LC-MS*. DOI: [10.17504/protocols.io.byhcpt2w](https://doi.org/10.17504/protocols.io.byhcpt2w).

